Applied Clay Science 251 (2024) 107326

Contents lists available at ScienceDirect

Applied Clay Science

journal homepage: www.elsevier.com/locate/clay

Research Paper

Implementing light elements detection and quantification in aluminosilicate materials using a Low-Z total-reflection X-ray fluorescence spectrometer

Ignazio Allegretta [a,*], Dragic Krstajic [b], Peter Wobrauschek [b], Peter Kregsamer [b], Dieter Ingerle [b,c], Christina Streli [b], Carlo Porfido [d], Roberto Terzano [d]

[a] Dipartimento di Scienze e Tecnologie Biologiche ed Ambientali, Università del Salento, via Monteroni 165, 73100 Lecce, Italy
[b] Atominstitut, TU Wien, Stadionallee 2, 1020 Vienna, Austria
[c] X-ray Center TU Wien, Lehargasse 6, 1060 Vienna, Austria
[d] Dipartimento di Scienze del Suolo, della Pianta e degli Alimenti, Università degli Studi di Bari Aldo Moro, Via G. Amendola 165/A, 70126 Bari, Italy

ARTICLE INFO

Keywords:
TXRF
Fluorine
Light elements
Clays
Rocks
Geochemistry

ABSTRACT

Total-reflection X-ray fluorescence (TXRF) is a well-established atomic spectroscopy technique used for the elemental characterization of different kinds of matrixes in several fields. Previous works demonstrated its applicability for the elemental quantification of aluminosilicates and, in particular, clays. However, one of the limits of the previously developed methods was the detection and quantification of light elements, in particular for those elements with an atomic number (Z) below 13 (Al).

In the present work a new TXRF-based analytical method for the quantification of light elements in aluminosilicate materials is described, using an in-house built Low-Z TXRF spectrometer equipped with a Cr source, a multilayer monochromator, an SDD detector equipped with an ultrathin Si_3N_4 window and a vacuum chamber. Samples were prepared as simple slurries (dispersing 50 mg of powder into 2.5 mL of 1%-Triton X-100 water solution and adding Ag as internal standard) and 10 μL were deposited onto a quartz carrier and dried before the analysis. Light elements such as F, Na and Mg were quantified with a limit of detection of 682, 260 and 133 mg/kg, respectively. Carbon and oxygen could also be detected. The new method allowed a complete analysis of major elements in aluminosilicates from F to Fe. The method showed a good accuracy in the range of 80–120% and the results agreed with the data obtained with a commercial TXRF spectrometer (for elements >13) and WDXRF, employed as reference methods. Despite a lower precision in respect to WDXRF, in some samples the quantification of F was possible only by using the Low-Z TXRF spectrometer. Finally, the method demonstrated to be suitable for the analysis of aluminosilicates, in particular when low amounts of sample (few milligrams) are available.

1. Introduction

Aluminosilicates are the most abundant natural minerals on Earth, being the main constituents of sediments and rocks. They are also of great economic and industrial importance in several fields, from building and construction to the food and pharmaceutical sectors. In addition, aluminosilicate materials can also be artificially synthetized for industrial purposes such as the production of ceramics, glasses, fibres, geopolymers, zeolites, etc. (Lopes et al., 2014). However, for applications in specific fields, aluminosilicates and aluminosilicate materials need to have well-defined characteristics, which must be assessed in advance to their use or commercialization. Among the chemical characteristics, the elemental composition is the first information usually needed since, together with other basic properties (i.e., crystalline structure), it allows the mineral identification and classification as well as helps researchers in the understanding of aluminosilicate genesis or history (usually in combination with petrographic and mineralogical data).

The quantification of Si, Al and Ca in argillites, marnes or other raw materials is important for the design of the kneading in the production of concrete (Kunther et al., 2017). The definition of the correct Si:Ca:Na

* Corresponding author.
E-mail address: ignazio.allegretta@unisalento.it (I. Allegretta).

https://doi.org/10.1016/j.clay.2024.107326
Received 15 September 2023; Received in revised form 22 January 2024; Accepted 26 February 2024
Available online 5 March 2024

ratio is mandatory for the preparation of soda-lime glasses (Martin, 2006). Besides, the presence of specific elements (chromophores) results in different glass colours (i.e., blue for Fe^{3+}, yellow for Fe^{2+}, violet for Mn^{3+}, etc.) (Carmona et al., 2009). Moreover, when geomaterials are used in food technology (i.e., bentonites, zeolites, etc.), it is mandatory to check the presence of potentially toxic elements (Abdelnaby et al., 2023). In the field of nanomaterials, a precise Ca:Mg:Si ratio is also requested for the correct synthesis of Mg-doped Si nanosheets (Okamoto et al., 2011). Aluminosilicate nanoparticles are also used in oil recovery or for the synthesis of new minerals, and the correct stoichiometric ratio among the elements should be assessed and measured before their application (Bing et al., 2022; Yahya et al., 2022). Elemental analysis is also necessary both for the processing of clay nanocomposites and for the monitoring of their efficiency in the remediation of polluted soils and waters as reviewed by Bosu et al. (2023), Han et al. (2019) and Lin et al. (2023). Finally, in archaeometrical studies, elemental analysis can shed light on the provenance of archaeological finds (ceramics, glass, stones, etc.) to help drawing the economic and social portrait of ancient communities (Hein et al., 2004).

Several analytical techniques are available for the elemental characterization of aluminosilicate materials, among which inductively coupled plasma sources associated with optical emission spectrometry (ICP-OES) or mass spectrometry (ICP-MS), atomic absorption spectrometry (AAS), neutron activation analysis (NAA) and X-ray fluorescence spectrometry (XRF) are the most used ones (Gutsuz et al., 2017; Hein et al., 2002, 2004; Ndzana et al., 2018).

Among the XRF techniques, in the recent years new analytical methods based on total-reflection X-ray fluorescence spectroscopy (TXRF) have been developed to analyse aluminosilicate materials with the aim of overcoming issues connected to sample availability and size (as in the case of cultural heritage studies, synthetic aluminosilicates, clay extraction from soils and sediments). In fact, the sample preparation for TXRF analysis usually requires lower amounts of samples (tens of milligrams) compared to other methods (from hundreds of milligram to grams). TXRF methods have been used for the analysis of minerals (Cherkashina et al., 2013), rocks and sediments (Cherkashina et al., 2014), clays (Allegretta et al., 2019) and ceramics (García-Heras et al., 1997, 2001; Maltsev et al., 2021, 2023). However, these methods do not allow the quantification of some light elements such as Na, Mg, Si and Al, which are very important in the study of aluminosilicates and aluminosilicate materials. Only in one of these studies (Allegretta et al., 2019), Si and Al were quantified, anyway leaving the problem of detecting or quantifying Na and Mg unsolved. Such analytical issues are related to two aspects: (i) the difficulty of light elements' fluorescence signal to emerge from the sample caused by both the self-absorption of the matrix and the absorption by the argon (Ar) gas present in the atmosphere; (ii) the use, in TXRF commercial instruments, of components which do not allow the proper excitation and detection of light elements, in favour of heavy elements. In fact, the fluorescence yields for light elements (Na, Mg, Al, etc) is very low (<4%) as far as their characteristic fluorescence energies (1–1.5 keV), thus high absorption will occur by the sample and by the air in ambient spectrometer. For this reason, the analysis of light elements requires vacuum conditions, a proper X-ray tube for efficient excitation of the light elements and a suitable detector to allow the efficient detection of the low energy fluorescence radiation.

Such difficulty to get information on light elements, in particular on major elements such as Na and Mg, makes TXRF an uncomplete technique for the comprehensive elemental analysis of aluminisolicate rocks and materials. For this reason other analytical techniques which can provide the quantification of both light and major elements are usually preferred, even if they need longer sample preparation procedures (ICP-AES, ICP-MS, AAS), the use of hazardous and polluting chemical (ICP-AES, ICP-MS, AAS), higher sample amounts (WDXRF) or longer analytical times (INAA).

However, the recent scientific and technological developments of TXRF spectrometers' components nowadays allow the detection and quantification of light elements, too. Excluding TXRF instrumentation developed at synchrotron radiation facilities, the first improvements of laboratory spectrometers for the detection of light elements dates back to the end of the '90s by Streli et al. (1989, 1993, 1995). In this first work, apart from the use of a vacuum system (which is mandatory to avoid the absorption of the light elements fluorescence signal by the atmospheric Ar), a TXRF spectrometer was implemented by using Cu or Cr X-ray sources, with the result of exciting light elements down to C. The implementation of the spectrometer with a 1300 W Cr source and a multilayer monochromator then allowed the best performances in terms of elements' sensitivity and limit of detection (Streli et al., 1995). Afterwards, other sources were used for the excitation of light elements (Mo-L, W-M, Si-Kα, Al-Kα), and even if better performances were obtained in terms of signal-to-noise ratio, one of the disadvantages was the loss of information on high-Z elements (Streli et al., 1997, 1999). To overcome this issue, Wobrauscheck et al. (2015) developed a spectrometer equipped with two low-power X-ray tubes: one with a Cr target for light elements and one with a Rh target for heavy elements. Prost et al. (2018) proposed a dual energy-band excitation with a Rh low power tube, consisting in the excitation of both low- and high-Z elements with Rh L-lines and K-lines, respectively, changing the excitation parameters (voltage and current). Another technological progress was the implementation of the spectrometers with a Si(Li) detector equipped with an ultrathin window having a 300 nm polymer windows on a supporting Si grid, resulting in an improved signal-to-noise ratio in the low energy range region, compared to silicon-drift detectors (SDDs) (Sasamori et al., 2009; Streli et al., 2004). Even though the technology of the spectrometers has been improved and prototype TXRF spectrometers have been assembled, their application on real samples and in particular on complex matrices has not been yet fully explored. Preliminary studies have been carried out on silicon wafers and water standard reference materials (Streli et al., 2004; Prost et al., 2015, 2018). Hoefler et al. (2006) investigated Mg in human cerebrospinal fluid and monitored the growth of bacteria biofilms checking the variation of C signal during 11 days of inoculation. To the Authors' knowledge, no other studies on the low-Z element analysis of complex samples and, in particular, aluminosilicates by TXRF are available.

For this reason, this work aims at implementing, for the first time, a TXRF method able to quantify light elements (such as F, Na and Mg) together with heavier elements in aluminosilicates and aluminosilicate materials, requiring only very small amounts of samples (tens of milligrams). To fulfil these objectives, a Low-Z TXRF spectrometer developed at the Atominstitut of the Technical University of Wien (Krstajic, 2022) was used. The analytical method was developed and validated, and the results were compared with those obtained with a commercial TXRF spectrometer and a WDXRF spectrometer, as reference method. The results of the present paper can be used for the development of new TXRF spectrometers capable of performing a complete analysis of all the most important elements in very small amounts of aluminosilicates and aluminosilicate samples.

2. Materials and methods

2.1. Reference materials for calibration and validation

A series of nine reference geomaterials distributed by SARM-CRPG (France) was selected for the calibration of the Low-Z TXRF spectrometer and the validation of the analytical method. These reference materials are all aluminosilicates with different Si/Al ratio and have a different elemental composition. They allowed calibrating and validating the method in different elemental concentration ranges. The calibration set consisted of six aluminosilicate samples: albite (AL-I), anorthosite (AN-G), basalt (BE-N), dolerite (WS-E), phlogopite (Mica-Mg) and serpentine (UB-N). Only certified values above the limit of detection (LOD) were considered for the calibration. The validation set was composed of other three certified reference geomaterials:

zinnwaldite (ZW-C), granite (GS-N) and diorite (DR-N).

2.2. Analysis with the Low-Z TXRF spectrometer

All the samples were prepared using a procedure slightly modified from that reported in Allegretta et al. (2019). Briefly, 50 mg of powder were poured into a plastic tube and dispersed in a 2.5 mL 1% Triton X-100 water solution. Fifty microlitres of Ag 1000 mg/L (Sigma Aldrich CHEMIE GmbH, Germany) standard solution were added to the slurry in order to achieve a final Ag concentration of 1000 mg/kg and the prepared slurries were suspended in an ultrasonic bath for 10 min. Differently from Allegretta et al. (2019), Ag was used instead of Se as internal standard, being the Se K-lines not detectable by the Low-Z TXRF spectrometer. Ag L-lines (2.98 keV), which overlap Ar-Kα from the air, can be easily detected under vacuum conditions as there is no Ar present. Then, the slurries were shaken again with a vortex for 30 s and 10 μL of the suspension were deposited with a micropipette onto a quartz reflector. Finally, the disks were placed on a heating plate (50 °C) under a laminar flow hood for drying. Three disks for each suspension were prepared and analysed for 1000 s of live time, each.

The analyses were carried out with a low-Z TXRF spectrometer developed by the Atominstitut of the Technical University of Wien (Austria) (Krstajic, 2022). The instrument is composed of a long fine focused Cr X-ray source (30 kV, 10 mA), a Ni/C monochromator, a beam collimating slit system and an Amptek C2 SDD detector equipped with an ultrathin Si_3N_4 window and a magnetic field electron trap to suppress the noise due to Auger-Meitner-, photo- and Compton electrons. Analyses were performed under vacuum (100 Pa) conditions. Acquisitions were done at half the critical angle of quartz (0.17°), which was determined each time during angle scan.

For the calibration, the sensitivity of Ag was considered equal to 1, and the relative sensitivity (S_r) of each element was determined as the slope of the line obtained by plotting the certified concentration versus the product N_eC_{is}/N_{is} where N_e is the net counts of the fluorescence peak of the element e, C_{is} and N_{is} are the concentration and the fluorescence's peak net counts of the internal standard, respectively. Peak deconvolution was performed using PyMCA (Solé et al., 2007).

After the calibration of the spectrometer with the calibration set, the samples of the validation set were analysed. For the validation, two parameters were studied: accuracy and precision. The accuracy was expressed in terms of recovery (R) in respect to the elements' concentration of the reference materials, expressed in percentage. The precision was defined in terms of relative standard deviation (%RSD). In addition, the limit of detection (LOD) for each studied element was determined according to Klockenkämper and von Bohlen (2015):

$$LOD = 3\frac{C_i}{N_{net}}\sqrt{N_{back}}$$

where C_i is the certified concentration of the i element, N_{net} and N_{back} are the net counts and the background underneath the peak, respectively.

2.3. Analyses with Mo-TXRF and WDXRF spectrometers

The results obtained with the Low-Z TXRF spectrometer were compared with those determined with WDXRF, as a reference analytical technique, and a commercial TXRF spectrometer.

For WDXRF analyses, samples were prepared as beads by mixing 5.0 g of powder with 2 mL of 2%$_{w/V}$ Elvacite® 2046 (PANalytical B.V., The Netherlands) solution in RPE grade acetone (Carlo Erba Reagenti Spa, Italy) in an agate mortar. After acetone evaporation, the mix was transferred into a 45 mm-aluminium cup containing 5.0 of boric acid (Carlo Erba Reagenti Spa, Italy). Then, samples were pressed (25 t for 5 min) to obtain uniform disks. The analyses were performed with a Supermini 200 WDXRF spectrometer (Rigaku Corporation, Japan). The instrument was equipped with a Pd source (50 kV, 4 mA), a Zr filter, a slit system, three analysing crystals (LiF, PET, and RX25), a scintillator detector, and a proportional counter. Analyses were performed under vacuum conditions (<12 Pa).

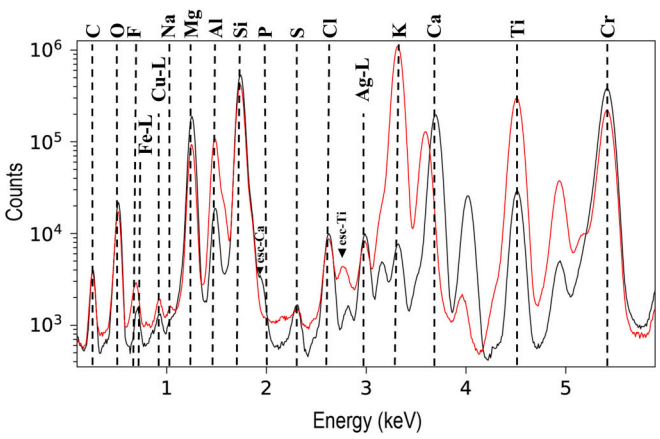

Fig. 1. TXRF spectra of the samples UB-N (black) and Mica-Mg (red) and the identified elements peaks. (For interpretation of the references to colour in this figure legend, the reader is referred to the web version of this article.)

A commercial TXRF spectrometer (Mo-TXRF) S2 Picofox (Bruker Nano GmbH, Germany) equipped with a Mo source (50 kV, 600 μA, 30 W) and a 30 mm^2 SDD (resolution <150 eV at Mn-Kα) was employed. Samples were prepared as described by Allegretta et al. (2019), and the analysis were performed for 1000 s of live time in air and under environmental pressure.

Student's t-test was used to compare the concentration values obtained with the Low-Z TXRF spectrometer and with the other two techniques. A confidence level of 95% was chosen. Before applying the t-test, Fisher F-test on the standard deviations was applied using, also in this case, a confidence value of 95%.

3. Results and discussion

3.1. Calibration of the Low-Z TXRF spectrometer

The first step of the study was to qualitatively understand which elements could be detected in this kind of samples with the Low-Z TXRF spectrometer. According to the literature, the analysis of light elements with a Low-Z TXRF spectrometer was never performed before on complex matrixes but only on water solutions (Prost et al., 2015, 2018). Fig. 1 clearly shows the complexity of the TXRF spectra of the two aluminosilicate samples (UB-N and Mica-Mg) used for the calibration of the spectrometer. In particular, the fluorescence K-lines of all the elements from Z = 6 (C) to Z = 24 (Cr) can be detected. The L-lines of Fe, Cu and Ag (added as internal standard) can be also observed. The Cu-signal comes from the electron trap (made of Cu). All those fluorescence lines were detectable because of a series of factors: i) the vacuum pump removed air nearby the sample, thus removing Ar interference; ii) the Si_3N_4 ultrathin window allowed the detection of the fluorescent signal of very light elements, including C; finally, iii) the Cr target as X-ray source (5.42 keV) together with a high power tube provided a better excitation of light elements with low energy fluorescence lines, as compared to the typical targets used in commercial TXRF instruments (Ag, Rh, Mo, etc) which, on their turn, provide a higher excitation energy (around 20 keV). The same detection capabilities cannot be achieved with commercially available TXRF spectrometers, which in the best case can detect only Al or Mg when they are present at high concentrations in this kind of matrices (Allegretta et al., 2019; Maltsev et al., 2021). The escape peaks of Ca and Ti can also be observed in the spectra.

For each spectrum of the calibration set, the limit of detection (LOD) was calculated and the average LOD of the detected elements is reported

Table 1
Limit of detection of the elements detected in the certified reference materials expressed as element and oxide concentrations.

LOD (mg/kg)											
Na	Mg	Al	Si	P	K	Ca	Ti	Fe	F	S	Cl
260	133	106	201	157	8	43	2	5526	682	15	5
Na_2O	MgO	Al_2O_3	SiO_2	P_2O_5	K_2O	CaO	TiO_2	Fe_2O_3			
350	220	200	430	360	10	60	4	7900			

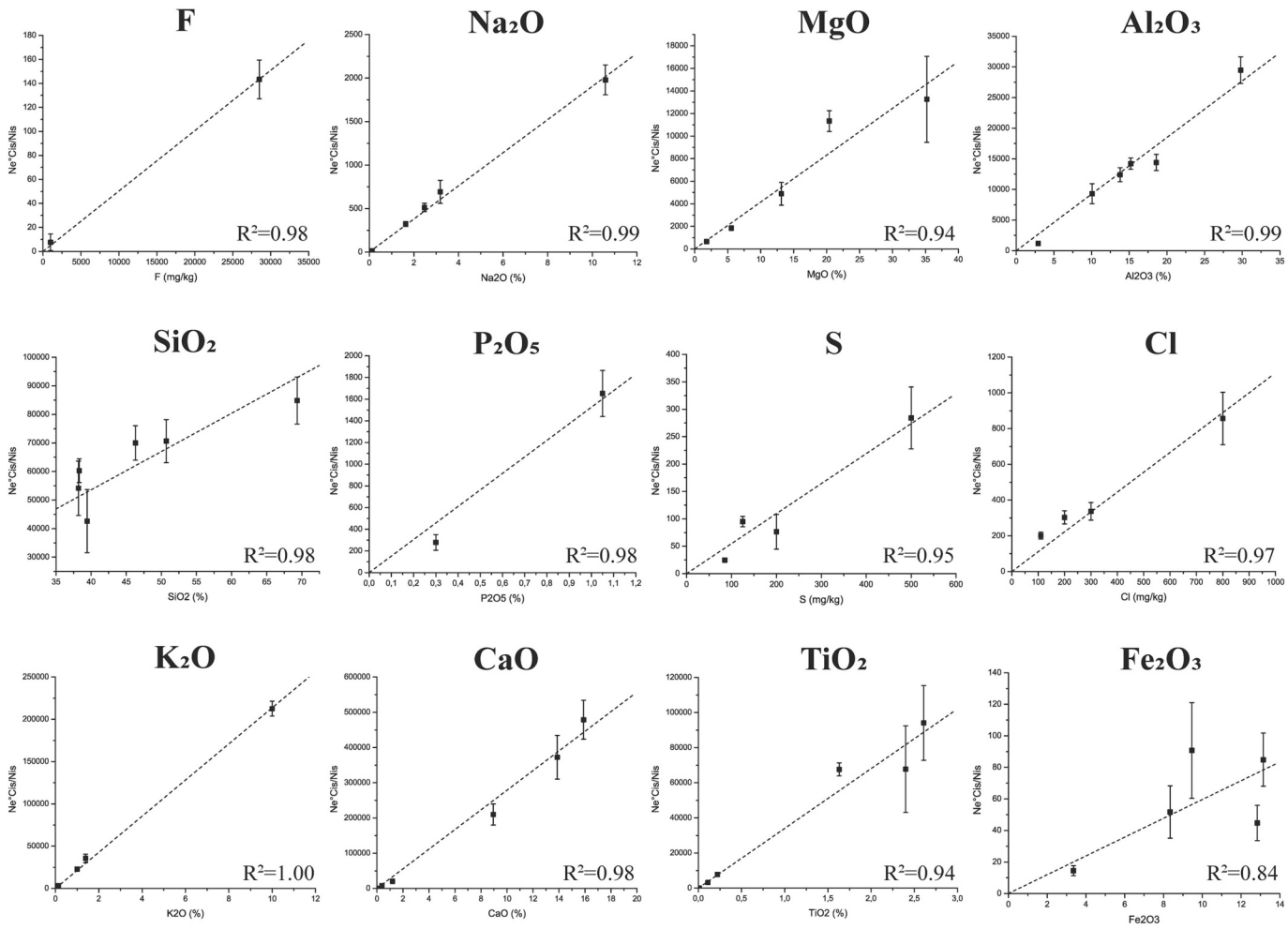

Fig. 2. Relative sensitivity calibration of the elements expressed as elements (for F, S and Cl) or oxides.

Table 2
Relative sensitivity (S_r) of the elements analysed with the Low-Z TXRF spectrometer.

S_r (for elements)											
F	Na	Mg	Al	Si	P	S	Cl	K	Ca	Ti	Fe
0.005034	0.051312	0.068872	0.174679	0.286952	0.433296	0.619055	1.26874	2.588742	3.89684	5.678461	0.000852

S_r (for oxides)								
Na_2O	MgO	Al_2O_3	SiO_2	P_2O_5	K_2O	CaO	TiO_2	Fe_2O_3
190.3684	415.297	924.05	1340.065	1523.102	21,357.12	27,862.41	34,042.37	5.960053

in Table 1.

Based on the certified concentrations of the elements in the reference materials used for the calibration set, the S_r of each element (F, Na, Mg, Al, Si, P, S, Cl, K, Ca, Ti and Fe) was determined in respect to Ag. Only the certified concentrations of the elements (and not just proposed) whose value was higher than the LOD were considered for the

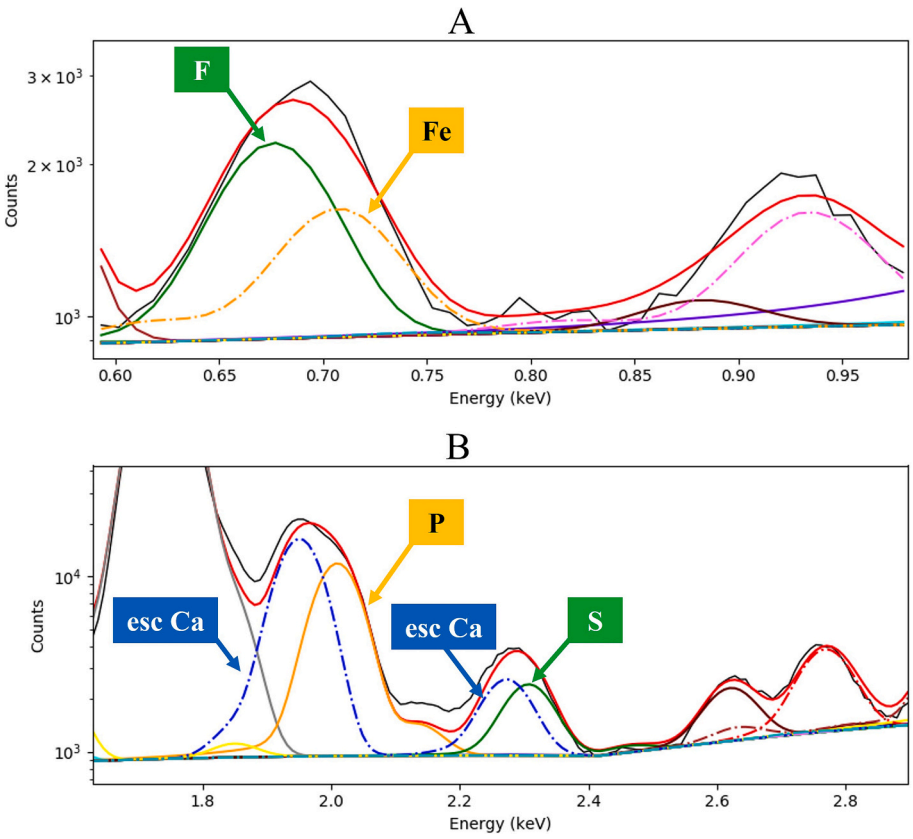

Fig. 3. (A) Fitting of the TXRF spectra of the Mica-Mg sample showing the overlapping of the F (green line) and Fe (dashed orange line) fluorescence peaks, and (B) fitting of the BE-N spectrum illustrating the effect of the Ca escape peaks (dashed blue line) on the deconvolution of P (orange line) and S (green line) fluorescence peaks. (For interpretation of the references to colour in this figure legend, the reader is referred to the web version of this article.)

Table 3
Quantification of the elements concentration in the reference materials DR-N, GS-N and ZW-C performed with the Low-Z TXRF spectrometer ($n = 3$).

Oxide	DR-N					GS-N					ZW-C				
	m	s	Cert	R	%RSD	m	s	Cert	R	%RSD	m	s	Cert	R	%RSD
	wt%			%		wt%			%		wt%			%	
Na_2O	2.93	0.70	2.99	98	24	4.17	0.29	3.77	111	7	0.46	0.09	0.33	139	20
MgO	4.08	0.86	4.40	93	21	2.45	0.12	2.30	107	5	0.14	0.03	0.16	87	21
Al_2O_3	15.66	3.14	17.52	89	20	15.21	0.65	14.67	104	4	20.99	3.83	18.45	114	18
SiO_2	51.94	11.67	52.85	98	22	73.22	4.74	65.80	111	6	61.78	2.43	54.00	114	4
P_2O_5	0.11	0.01	0.25	42	11	0.12	0.02	0.28	44	17	<LOD	–	0.03	–	–
K_2O	1.70	0.23	1.70	100	14	4.98	0.10	4.63	108	2	7.93	1.56	7.72	103	20
CaO	5.73	1.04	7.05	81	18	2.36	0.12	2.50	94	5	0.35	0.07	0.37	94	20
TiO_2	1.01	0.15	1.09	93	15	0.81	0.03	0.68	119	4	0.05	0.01	0.05	100	20
Fe_2O_3	11.20	2.57	9.7	115	23	3.63	0.48	3.75	97	13	14.72	2.96	9.46	156	20

Element	DR-N					GS-N					ZW-C				
	m	s	Cert	R	%RSD	m	s	Cert	R	%RSD	m	s	Cert	R	%RSD
	mg/kg			%		mg/kg			%		mg/kg			%	
F	<LOD	–	500	–	–	998	48	1050	95	5	54,794	10,031	54,500	101	18
S	299	26	350	86	11	151	14	140	108	9	340	82	300	113	24
Cl	417	58	400	104	14	524	16	450	116	3	118	2	30	393	2

m = average.
s = standard deviation.
Cert = certified value.
R = recovery.
%RSD = relative standard deviation.

calibration. Only in the case of S, for which element the concentrations were not certified, the proposed value was considered for S_r calculation. The lack of information about the concentrations of C and O in the reference materials made the determination of the S_r of these two elements not possible. All the calibration curves are shown in Fig. 2 and the calculated S_r values are reported in Table 2, expressed both for oxides and elements. The regression coefficient (R^2) ranged between 0.94 and 1.00, with the only exception of Fe, because the less sensible L-lines were considered, also partially overlapping with F K-lines. Indeed, fluorine was detected only in BE-N and Mica-Mg and the two points which deviate from linearity in the Fe_2O_3 calibration curve are exactly related to these two reference materials (Fig. 2), confirming the issue of the Fe L-line peak deconvolution when the F fluorescence peak is also present (Fig. 3A). Another issue may occur when Ca concentration is very high. In this case, Ca escapes peaks of both Kα and Kβ can emerge with an intensity equal to or higher than the fluorescence peaks of P and S, respectively, increasing the LOD of these two elements (Fig. 3B).

3.2. Method validation

After the calibration of the relative sensitivity, the validation of the method was performed by the analysis of the three reference materials: ZW-C, GS-N and DR-N. As shown in Table 3, the recovery (R) is in the range 80–120% for all the major elements, with the only exceptions of P_2O_5 in DR-N and GS-N, and Na_2O and Fe_2O_3 in ZW-C. The wrong estimation of P_2O_5 concentration could be attributed to the high intensity of the Ca Kα escape peak (see previous paragraph). In the sample ZW-C, the certified concentration was lower than the LOD of P_2O_5, and for this reason it couldn't be quantified even if the CaO concentration was very low (0.35 wt%). The strong F fluorescence peak in ZW-C (the concentration of F in this sample is 5.45 wt%), which overlaps the less intense peak of Fe L-lines, do not allow obtaining a good accuracy for Fe_2O_3 (see previous paragraph). In the case of Na_2O, the certified concentration for ZW-C is 0.33 ± 0.10 mg/kg but, considering that statistically the real value is within three standard deviations, the quantification obtained with the Low-Z TXRF spectrometer could be considered acceptable, even if the Na_2O concentration for this reference material cannot be considered accurate. Differently, in the other two reference materials the recovery is about 98 and 111%, which means that Na_2O is accurately quantified. A good accuracy was obtained for all the minor elements (F, S and Cl), with the only exception of Cl in sample ZW-C, where the recovery was 393%. In this case, the certificate of analysis reported only a proposed value (30 mg/kg) with no standard deviation, therefore we cannot completely rely on it.

Despite the good accuracy of the method, the %RSD is often >10% for all the elements, resulting in a low precision of the method. In general, geological samples are multiphase and not homogeneous materials and this can lead to a variable deposition of the powder onto the quartz disk, which may result in locally-enriched or -depleted areas for some elements. Only in the case of the sample GS-N, %RSD is lower than 10%, demonstrating a good precision, with the exception of P_2O_5 and Fe_2O_3.

3.3. Comparison with other analytical techniques

The results obtained with the Low-Z spectrometer were compared with those obtained with a widely-used commercial instrument (Bruker S2 Picofox, Mo-TXRF) and with a WDXRF spectrometer (Table 5). It is important to underline that, individually, the two TXRF spectrometers cannot providethe complete information about the elemental composition of all the most important elements in aluminosilicates. In fact, the Low-Z TXRF spectrometer does not allow the P_2O_5 (as discussed in the previous paragraphs) and MnO quantification. For MnO, the problem is that aluminosilicates do not usually contain very high amounts of MnO and its concentration is not enough to allow the Mn L-lines (0.637 keV) to emerge from the baseline. On the contrary, the excitation of the Mn K-lines, which are more sensitive than L-lines, by the Mo target installed on

Table 4
Summary of the methods used for the quantification of fluorine in aluminosilicates.

Paper	Method	Description	Performances
Ingram (1970)	Potentiometry (specific ion electrode)	Sample preparation: heat a mixture of 100 mg of sample, 500 mg $NaCO_3$, 100 mg ZnO at 900 °C for 30 min. Add 30 mL of water and steam-bath for overnight. Filter with Whatman n.42 and dilute with a 6 M HCl. Remove CO_2 and dilute with water. Dilute 10 mL with 10 mL of 0.2 M sodium citrate-0.2 M potassium nitrate solution. Analysis: Measure the potential with the fluoride electrode.	Fluorine concentration: from 250 mg/kg to 5.72%; LOD: N.A.; One day for the preparation of the sample; 15 min for the analysis.
Jagner and Pavlova (1972)	Titration	Sample preparation: the same of Ingram (1970). Analysis: Standard addition titration adding NaF solution and recording the potential after equilibrium.	Fluorine concentration: 180–250 mg/kg; LOD: N.A.; One day for the preparation of the sample; 15 min for the analysis.
Havránek et al. (2004)	INAA	Sample preparation: none. Analysis: Irradiation of the sample with fast neutron fluence rates of $9{\cdot}10^{13}$ and $2{\cdot}10^{13}$ n·cm^{-2} s^{-1}. Counting time of 10, 15 and 20 s.	Fluorine concentration: 500 mg/kg; LOD: at least 1000 mg/kg; No sample preparation; Few minutes for the analysis
	RPAA	Sample preparation: alkaline-oxidative fusion (500 mg NaOH, 7 g Na_2O_2 at 900 °C for 2 min), dissolution with H_2SO_4, extraction with Zr-DEHPA in hexane, addition of H_2SO_4, fluorine strimming with NH_4OH + acetone+tributylphosphate. Analysis: Irradiation at 20 MeV for 5 h.	Fluorine concentration: N.A.; LOD: 0.5 mg/kg estimated on biological sample; 30 min for the sample preparation; 5–8 h for the analysis.
	PIGE	Sample preparation: none. Analysis: Irradiation of the sample for 4–10 min with a proton fluence between 3 and 30 μC.	Fluorine concentration 471 mg/kg; LOD: 4–6 mg/kg; No sample preparation; Few minutes for the analysis.
Kuz'mina et al. (2023)	WDXRF	Sample preparation: 1) Fusion: 150 mg of sample, 600 mg lithium metaborate, 1.2 g lithium tetraborate at 1050 °C for 12 min. Grind the sample and add ethanol and press into a 3 cm-diameter tablet. 2) Pressing: 300 mg of sample, 60 mg of polystyrene. Grind, add ethanol and press into a 3 cm-diameter tablet. Analysis: AXIOS WDXRF (PANanalytical B.V.) Rh source (3 kW, 30 mA, 100 kV), proportional and scintillator counters.	Fluorine concentration: from 0.13 to 6.9% LOD: 700 mg/kg for fusion, 200 mg/kg for pressing. 30 min for the sample preparation; Few minutes for the analysis (only fluorine concentration).

(continued on next page)

Table 4 (*continued*)

Paper	Method	Description	Performances
This work	TXRF (Low-Z TXRF Spectrometer)	Sample preparation: 50 mg of sample dispersed into 2.5 mL of 1% Triton X-100 solution, 50 μL of Ag standard solution (1000 mg/L). Deposition of 10 μL of suspension on a quartz reflector and drying on a heating plate. Analysis: Low-Z TXRF spectrometer with a Cr source (300 W, 10 mA, 30 kV), Amptek C2 SDD detector equipped with an ultrathin Si_3N_4 window.	Fluorine concentration: 0.1–5.5%; LOD: 682 mg/kg; Few minutes for the sample preparation; 17 min for the analysis (for all the elements)
	WDXRF	Sample preparation: 5 g of sample mixed with 2 mL of 2%*w/V* Elvacite® 2046 in acetone. Pressing into 45 mm-aluminium cup. Analysis: Supermini 200 EDXRF spectrometer (Rigaku), Pd source, (200 W, 4 mA, 50 kV), proportional and scintillator counters.	Fluorine concentration: 4.5% LOD: 4856 mg/kg Few minutes for the sample preparation; Few minutes for the analysis (only fluorine concentration).

the commercial instrument allowed the correct quantification of MnO. On the other hand, the Mo-TXRF spectrometer cannot quantify light elements such as Na, F, S and, when the concentration is very low (i.e. ZW-C), also not Mg. This is mainly connected to the configuration of the spectrometer which does not work under vacuum and is not equipped with both a sensitive detector for light elements and a source which can efficiently excite these elements. Even if the quantification of P_2O_5 was performed, it is quite far from the certified concentrations (0.35 wt% for DR-N and 0.26 wt% for GS-N). In addition, in this case, the overlapping with the Ca escape peak hindersthe correct deconvolution of the P fluorescence peak. For S, the problem is due to the overlapping of the Mo L-lines, the presence of Ca escape peaks and an increase in the background in this spectral region (Allegretta et al., 2019). This last aspect also affects the quantification of Cl, in particular in ZW-C sample, where Cl concentration is lower than in the other reference materials (the proposed value is 30 mg/kg). WDXRF can detect and quantify all the elements, including P, which was not correctly quantified with both TXRF spectrometers. Indeed, the results for P_2O_5 are accurate considering the certified values of 0.25, 0.28 and 0.025 wt% for DR-N, GS-N and ZW-C, respectively. This is due to the lack of Ca escape peaks in WDXRF spectra. In fact, the formation of escape peaks is connected with energy-dispersive XRF systems and not with wavelength-dispersive XRF instruments (Beckhoff et al., 2006). Fluorine was only quantified in ZW-C while in the other samples it was not detected. Differently, F could be quantified in both ZW-C and GS-N with the Low-Z TXRF instrument, showing a lower detection limit for F compared to the WDXRF system (4856 mg/kg). The possibility of quantifying fluorine in aluminosilicates with TXRF is very important, because there are very few methods capable of performing this kind of analysis (Table 4). WDXRF is one of these methods but, according to the sample preparation startegy, it can require from 150 mg to 5 g of material. The preparation of fused beads generally leads to higher limits of detection than pressed pellets. Kuz'-mina et al. (2023) quantified them as 700 and 200 mg/kg, respectively. However, they determined the LOD on pure fluoride samples (NaF, CaF_2 and MgF_2) thus allowing a lower LOD. Using of a WDXRF with a higher source power respect to the one used in the present paper could reduce the WDXRF LOD, because a more intense signal is produced in the same time of analysis. Among other methods for the quantification of F in aluminosilicates, Havránek et al. (2004) tested instrumental neutron activation analysis (INAA), photon activation analysis with radiochemical separation (RPAA) and photon induced γ-ray emission (PIGE). With INAA, 100–150 mg of sample were used and the analysis lasted maximum 30 s. However, the overlap of the ^{28}Al activity increased the LOD according to the Al concentration, which of course is a big problem in aluminosilicates. On the contrary, with RPAA, F signal did not suffer any interference and the LOD was 1–2 mg/kg. However, the sample preparation was quite complex and the analyses lasted for hours. Finally, only using PIGE, Havránek et al. (2004) were able to quantify F in a soil sample obtaining a LOD of 4–6 mg/kg. Fluorine can be measured also using a specific ion electrode (Ingram, 1970) or by titration (Jagner and Pavlova, 1972). Even if these methods allow the quantification of very low concentrations of F (from 40 to 800 mg/kg), in both cases a very complex and time-consuming extraction procedure is required (Table 4). The present TXRF method is surely faster than these methods and even if the LOD for F is higher compared to PIGE and the two above-cited chemical methods, its performances are better than WDXRF and the

Table 5
Comparison of the results obtained with the Low-Z TXRF. Mo-TXRF and WDXRF spectrometers. Results are expressed in terms of average concentration ± standard deviation ($n = 3$).

Oxide	DR-N			GS-N			ZW-C		
	Low-Z TXRF	Mo-TXRF	WDXRF	Low-Z TXRF	Mo-TXRF	WDXRF	Low-Z TXRF	Mo-TXRF	WDXRF
	wt%								
Na_2O	2.93 ± 0.70 $^{\#}$	–	2.78 ± 0.44	4.17 ± 0.29 $^{\#}$	–	3.70 ± 0.60	0.46 ± 0.09 $^{\#}$	–	0.26 ± 0.02
MgO	4.08 ± 0.86 $^{*,\#}$	4.94 ± 0.30	5.21 ± 0.03	2.45 ± 0.12 $^{*,\#}$	2.02 ± 0.21	2.85 ± 0.02	0.14 ± 0.03 $^{\#}$	–	0.09 ± 0.00
Al_2O_3	15.66 ± 3.14 $^{*,\#}$	16.60 ± 0.95	15.84 ± 1.89	15.21 ± 0.65 $^{*,\#}$	15.44 ± 0.31	15.57 ± 0.34	20.99 ± 3.83 $^{*,\#}$	22.10 ± 1.40	19.20 ± 0.03
SiO_2	51.94 ± 11.67 $^{*,\#}$	51.69 ± 3.09	52.96 ± 0.82	73.22 ± 4.74 $^{*,\#}$	67.24 ± 2.54	68.14 ± 0.53	61.78 ± 2.43	48.60 ± 3.20	55.30 ± 0.38
P_2O_5	–	0.40 ± 0.09	0.24 ± 0.00	–	0.11 ± 0.02	0.26 ± 0.00	–	–	0.02 ± 0.00
K_2O	1.70 ± 0.23 $^{*,\#}$	1.67 ± 0.09	1.66 ± 0.07	4.98 ± 0.10 *	4.70 ± 0.12	4.54 ± 0.02	7.93 ± 1.56 $^{*,\#}$	8.60 ± 0.40	7.88 ± 0.01
CaO	5.73 ± 1.04 $^{*,\#}$	7.11 ± 0.43	6.29 ± 0.62	2.36 ± 0.12 $^{*,\#}$	2.48 ± 0.07	2.16 ± 0.01	0.35 ± 0.07 $^{*,\#}$	0.33 ± 0.02	0.32 ± 0.01
TiO_2	1.01 ± 0.15 $^{*,\#}$	1.10 ± 0.08	1.13 ± 0.01	0.81 ± 0.03	0.67 ± 0.05	0.65 ± 0.01	0.05 ± 0.01 $^{\#}$	–	0.05 ± 0.00
MnO	–	0.22 ± 0.02	0.21 ± 0.00	–	0.05 ± 0.00	0.06 ± 0.00	–	0.90 ± 0.10	0.96 ± 0.00
Fe_2O_3	11.20 ± 2.57 $^{*,\#}$	9.81 ± 1.27	10.22 ± 0.37	3.63 ± 0.48 $^{*,\#}$	3.71 ± 0.16	4.02 ± 0.09	14.72 ± 2.96 $^{*,\#}$	8.80 ± 0.50	10.49 ± 0.11

Element	mg/kg							
F				998 ± 48			54,794 ± 10,031$^{\#}$	44,900 ± 1970
S	299 ± 26		372 ± 4	151 ± 14$^{\#}$		173 ± 6	340 ± 82$^{\#}$	289 ± 2
Cl	417 ± 14*	397 ± 24	508 ± 12	524 ± 16*	454 ± 53	464 ± 11	118 ± 2	71 ± 4

* 95% confidence level (Low-Z TXRF vs Mo-TXRF).
$^{\#}$ 95% confidence level (Low-Z TXRF vs WDXRF).

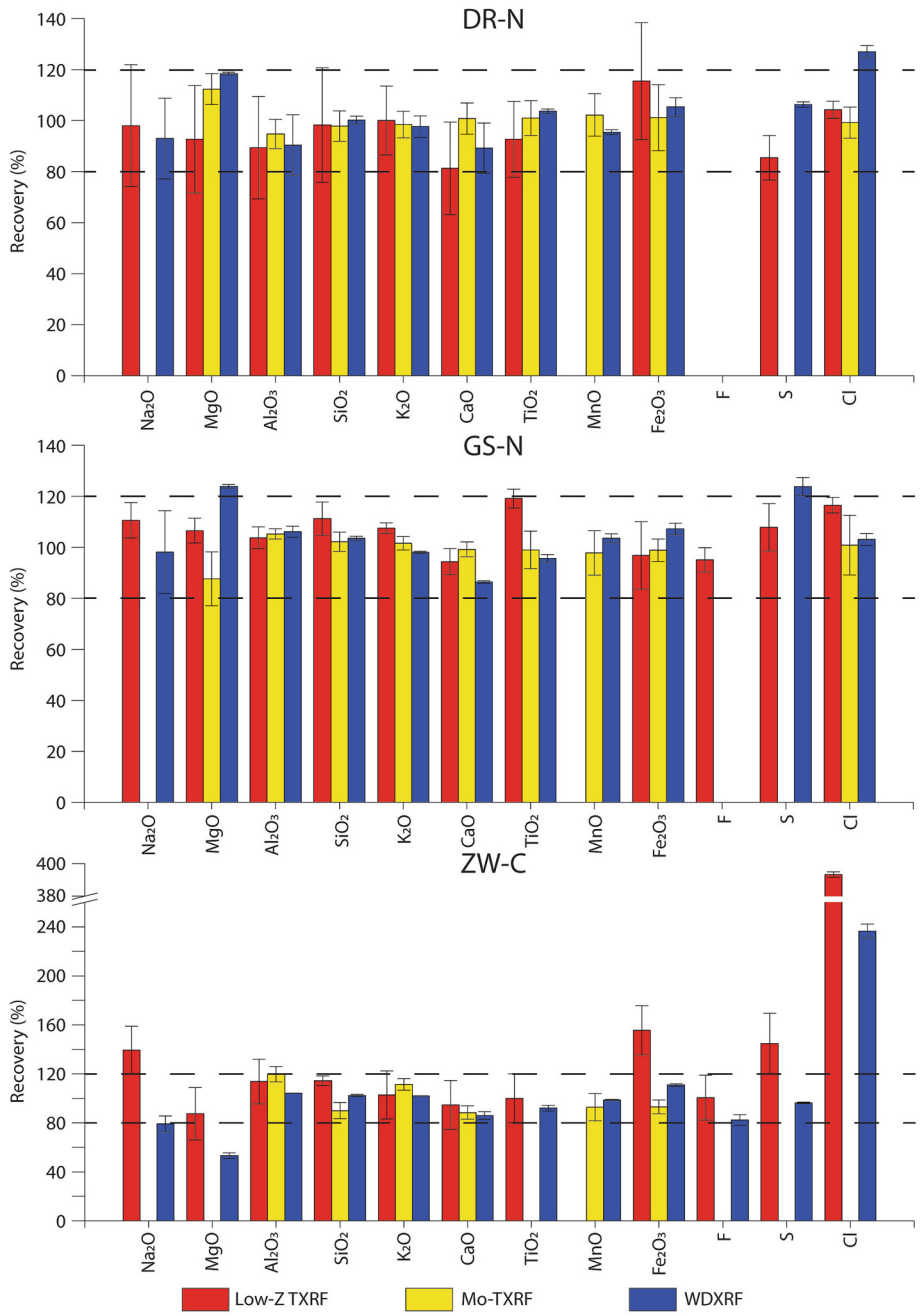

Fig. 4. Comparison of the recovery obtained with the three spectrometers for the analysis of the samples DR-N, GS-N and ZW-C.

other neutron spectroscopies (Table 4). Last but not the least, with TXRF the amount of sample needed is only 50 mg, much lower than the amount required for all the other methods (Table 4).

In general, the results produced with the two TXRF spectrometers show higher standard deviations compared to WDXRF. This can be explained by the very different amount of sample used for the analyses. In fact, for TXRF only 50 mg of material were used for the preparation of the suspension, from which just few microlitres were deposited on the reflector. On the contrary, in the case of WDXRF, 5 g of powder were employed (100 times more) and a large area (≈7 cm^2) of the bead was analysed, thus reducing the variability caused by the well-known heterogeneity of geological samples.

To compare the average elemental concentrations obtained with the Low-Z TXRF spectrometer with the data obtained with the other two methods, Student's *t*-test was used as a statistical tool (Table 5). The average concentrations obtained with the Low-Z TXRF spectrometer can be considered significantly comparable to those determined with the other spectrometers, with a 95% of confidence level. This result suggests that the Low-Z TXRF spectrometer can be successfully used for the chemical characterization of aluminosilicates, as an alternative to WDXRF, which is the reference analytical technique in this field. In terms of accuracy, the recovery calculated for all the quantified elements with the three analytical methods are quite similar. For MgO, Al_2O_3, SiO_2, K_2O, CaO, TiO_2 and Fe_2O_3, all the three methods showed a recovery in the range 80–120% (Fig. 4). Chlorine was overestimated with WDXRF in DR-N and with both WDXRF and Low-Z TXRF in ZW-C. A low accuracy was observed for Na_2O in ZW-C using both Low-Z TXRF and WDXRF. MgO was overestimated in the case of GS-N by WDXRF. Finally, Fe_2O_3 was overestimated with the Low-Z TXRF spectrometer in the case of ZW-C, which was caused by the overlapping of the strong F fluorescence peak in this sample. However, Fig. 4 pointed out that a good recovery was obtained for Fe_2O_3 in ZW-C by using Mo-TXRF. Moreover,

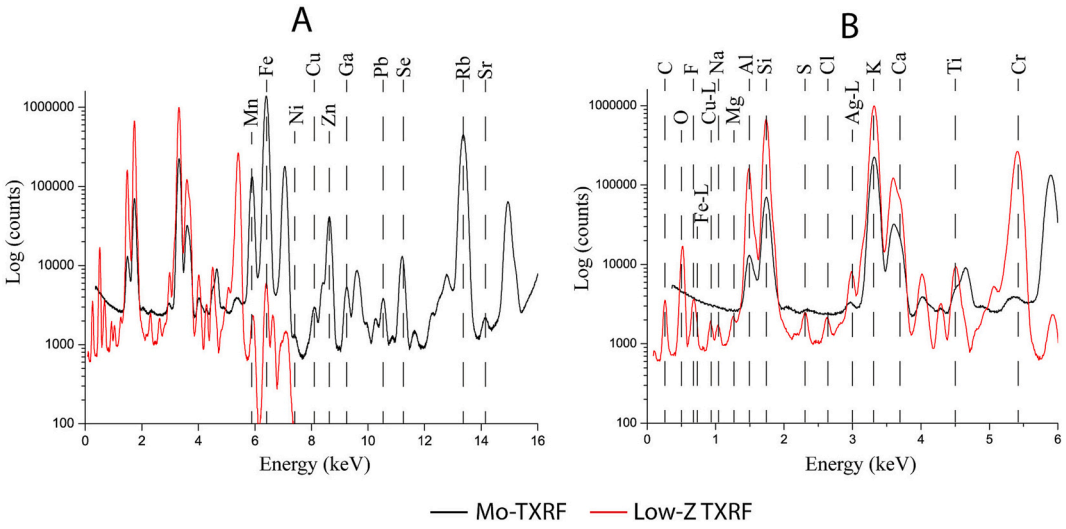

Fig. 5. (A) Comparison of the TXRF spectra of ZW-C acquired with both the Mo-TXRF instrument (black) and the Low-Z TXRF spectrometer (red). (B) Magnification of the two spectra in the range 0–6 keV. (For interpretation of the references to colour in this figure legend, the reader is referred to the web version of this article.)

Mo-TXRF allowed to accurately quantify also MnO which cannot be determined with the Low-Z TXRF spectrometer. Fig. 5 shows side-by-side the spectra obtained with the Low-Z TXRF spectrometer and with the Mo-TXRF instrument. It is evident that the two devices provide different pieces of information on the chemical composition of the same sample, and therefore could be used jointly for a complete analysis of aluminosilicates, for both major and minor elements. The fluorescence signal from 5.89 keV (Mn) to 16 keV could be recorded by using the Mo-TXRF instrument (Fig. 5A), giving information on elements not considered in the present work, such as Ni, Cu, Zn, Ga, Pb, Se, Rb and Sr. Besides, the Low-Z TXRF spectrometer could be used to collect the fluorescence signals below 6 keV (Fig. 5B), providing information on the major light elements. Indeed, only the Low-Z TXRF spectrometer allows recording a spectrum below the Al-Kα fluorescence signal.

3.4. Strategies for instrumental implementation

Practically, the issues related to the detection and quantification of Mn and Fe with the Low-Z TXRF spectrometer could be overcome by installing a second X-ray tube (such as Rh or Mo) on the spectrometer in order to excite the K-lines of Mn and Fe. Such a spectrometer would allow the full elemental composition of aluminosilicate materials to be quantified, alike WDXRF. Spectrometers equipped with two targets (Mo and W bremsstrahlung) are already available on the market and in this case the second target (W) is usually used for the excitation of the K-lines of heavy elements (i.e., Cd, Ag, Sn, etc). Wobrauschek et al. (2015) proposed a TXRF spectrometer equipped with a Rh and a Cr source providing good results for the analysis of water solutions. The same configuration could be proposed for the analysis of aluminosilicates and in general for complex matrixes.

Other strategies for the analysis of both light and heavy elements with TXRF consisted in the use of both K and L-lines of a Rh target (Prost et al., 2018) for elements excitation. Even if good results were obtained on water solutions (the lightest detected element being Na), preliminary studies (data not shown) on aluminosilicate materials did not give encouraging results to consider further its applicability to this kind of matrix. An explanation might be the fact that in this spectrometer a not monochromatized Rh-L radiation was used for the excitation, but a reflected pink beam cut-off above the Rh-L radiation. This led to a higher background, especially when using this type of matrices. Despite the better performances of WDXRF (which remains the main analytical tool for the elemental characterization of geological samples) for the analysis of aluminosilicate materials, as demonstrated by Allegretta et al. (2019), TXRF can be successfully used when only low amounts of sample are available (about 100 times less than the amount used for WDXRF). In this sense, TXRF spectrometry is suggested for quantification of elements, both light and heavy, in those fields in which the sample availability can be a problem such as for example, cultural heritage studies, mineral and material synthesis, clay characterization, sorption-desorption studies, etc.

4. Conclusions

In the present work, a new method based on TXRF for the detection and quantification of light elements in aluminosilicates and aluminosilicate materials was developed. The main findings can be summarized as follows:

- For the quantification of light elements in complex matrixes, a particular instrument equipped with a vacuum chamber, a Cr source, a multilayer monochromator and an SDD detector with an Si_3N_4 window was needed.
- Quantification of light elements from fluorine (F) to iron (Fe) in aluminosilicates was achieved as well as detection of carbon (C) and oxygen (O).
- Manganese (Mn) and other heavier elements could not be quantified, but the implementation of the spectrometer with a second X-ray source (i.e., Rh, Mo, etc) could overcome this problem.
- For the first time, TXRF was successfully used for the quantification of light elements in a complex matrix. In fact, to the authors' knowledge, only tests on water solution have been performed before. This is an important step, because it opens the possibility to analyse light elements not only in aluminosilicate materials, but also in other complex matrixes such as composites, soils, sediments, ores, and other environmental and biological samples.
- Compared to other methods (titration, potentiometry and RPAA), fluorine can be quantified in a faster way, without performing extraction, using a very simple sample preparation and with limits of detection comparable to PIGE and WDXRF.
- The present method required only 50 mg of sample, making this method applicable to fields in which the procurement of sufficient amounts of sample could be difficult (cultural heritage, archaeology, microsynthesis, sorption-desorption tests, etc).

CRediT authorship contribution statement

Ignazio Allegretta: Conceptualization, Data curation, Formal analysis, Funding acquisition, Investigation, Methodology, Project administration, Software, Validation, Visualization, Writing – original draft, Writing – review & editing. **Dragic Krstajic:** Data curation, Investigation, Software, Validation. **Peter Wobrauschek:** Investigation, Methodology, Software, Validation, Writing – review & editing. **Peter Kregsamer:** Methodology, Writing – review & editing. **Dieter Ingerle:** Software, Writing – review & editing. **Christina Streli:** Funding acquisition, Project administration, Resources, Supervision, Writing – review & editing. **Carlo Porfido:** Investigation, Writing – review & editing. **Roberto Terzano:** Funding acquisition, Project administration, Resources, Supervision, Writing – original draft, Writing – review & editing.

Declaration of competing interest

The authors declare that they have no known competing financial interests or personal relationships that could have appeared to influence the work reported in this paper.

Data availability

No data was used for the research described in the article.

Acknowledgements

This work was developed in the frame of COST Action CA18130 ENFORCE TXRF supported by COST (European Cooperation in Science and Technology). This study was also carried out within the Agritech National Research Center and received funding from the European Union Next-GenerationEU (PIANO NAZIONALE DI RIPRESA E RESILIENZA (PNRR) MISSIONE 4 COMPONENTE 2, INVESTIMENTO 1.4 D.D. 1032 17/06/2022, CN00000022). This manuscript reflects only the authors' views and opinions, neither the Europena Union nor the European Commission can be considered responsible for that.

References

Abdelnaby, A., Abdelaleem, N.M., Elshwy, E., Monsour, A.H., Ibrahim, S.S., 2023. Application of bentonite clay, date pit and chitosan nanoparticles as promising adsorbents to sequester toxic lead and cadmium from milk. Biol. Trace Elem. Res. 201, 2650–2664. https://doi.org/10.1007/s12011-022-03353-w.

Allegretta, I., Ciasca, B., Pizzigallo, M.D.R., Lattanzio, V.M.T., Terzano, R., 2019. A fast method for the chemical analysis of clays by total-reflection x-ray fluorescence spectroscopy (TXRF). Appl. Clay Sci. 180, 105201 https://doi.org/10.1016/j.clay.2019.105201.

Beckhoff, B., Kanngiesser, B., Langhoff, N., Wedell, R., Wolff, H., 2006. Handbook of Practical X-Ray Fluorescence Analysis. Springer, Berlin Heidelberg.

Bing, L., Sheng, M., Sun, J., Zhai, C., Bai, S., 2022. Physicochemical characteristics and growth mechanisms of the aluminosilicate nanoparticles for synthesis of clinoptilolite. Chem. Select 7. https://doi.org/10.1002/slct.202201172.

Bosu, S., Rajamohan, N., Lam, S.S., Vasseghian, Y., 2023. Environmental remediation of agrochemicals and dyes using clay nanocomposites: review on operation conditions, performances, evaluation, and machine learning applications. Rev. Environ. Contam. Toxicol. 261, 17. https://doi.org/10.1007/s44169-023-00043-z.

Carmona, N., Villegas, M.A., Jimenez, P., Navarro, J., Garcia-Heras, M., 2009. Islamic glasses from Al-Andalus. Characterisation of materials from a Murcian workshop (12th century AD, Spain). J. Cult. Herit. 10, 439–445. https://doi.org/10.1016/j.culher.2008.12.005.

Cherkashina, T.Yu., Panteeva, S.V., Finkelshtein, A.L., Makagon, V.M., 2013. Determination of Rb, Sr, Cs, Ba, and Pb in K-feldspars in small sample amounts by total reflection X-ray fluorescence. X-Ray Spectrom. 42, 207–212. https://doi.org/10.1002/xrs.2469.

Cherkashina, T.Yu., Panteeva, S.V., Pashkova, G.V., 2014. Applicability of direct total reflection X-ray fluorescence spectrometry for multielement analysis of geological and environmental objects. Spectrochim. Acta B 99, 59–66. https://doi.org/10.1016/j.sab.2014.05.013.

García-Heras, M., Fernandez-Ruiz, R., Tornero, J.D., 1997. Analysis of archaeological ceramics by TXRF and contrasted with NAA. J. Archaeol. Sci. 24, 1003–1014.

García-Heras, M., Blackman, M.J., Fernández-Ruiz, R., Bishop, R.L., 2001. Assessing ceramic compositional data: a comparison of total reflection x-ray fluorescence and instrumental neutron activation analysis on late iron age Spanish celtiberian ceramics. Archaeometry 43, 325–347. https://doi.org/10.1111/1475-4754.00020.

Gutsuz, P., Kibaroğlu, M., Sunal, G., Hacıosmanoğlu, S., 2017. Geochemical characterization of clay deposits in the Amuq Valley (Southern Turkey) and the implications for archaeometric study of ancient ceramics. Appl. Clay Sci. 141, 316–333. https://doi.org/10.1016/j.clay.2017.03.004.

Han, H., Rafiq, M.K., Zhou, T., Xu, R., Masek, O., Li, X., 2019. A critical review of clay-based composites with enhanced adsorption performance of metal and organic pollutants. J. Hazard. Mater. 369, 780–796. https://doi.org/10.1016/j.jhazmat.2019.02.003.

Havránek, V., Kučera, J., Řanda, Z., Voseček, V., 2004. Comparison of fluorine determination in biological and environmental samples by NAA, PAA and PIXE. J. Radioanal. Nucl. Ch. 259, 325–329. https://doi.org/10.1023/B:JRNC.0000017312.00776.e5.

Hein, A., Tsolakidou, A., Iliopoulos, I., Mommsen, H., Buxeda i Garrigòs, J., Montana, G., Kilikoglou, V., 2002. Standardisation of elemental analytical techniques applied to provenance studies of archaeological ceramics: an inter laboratory calibration study. Anal. The 127, 542–553. https://doi.org/10.1039/b109603f.

Hein, A., Day, P.M., Cau Ontiveros, M.A., Kilikoglou, V., 2004. Red clays from Central and Eastern Crete: geochemical and mineralogical properties in view of provenance studies on ancient ceramics. Appl. Clay Sci. 24, 245–255. https://doi.org/10.1016/j.clay.2003.07.009.

Hoefler, H., Streli, C., Wobrauschek, P., Ovari, M., Zaray, Gy, 2006. Analysis of low Z elements in various environmental samples with total reflection X-ray fluorescence (TXRF) spectrometry. Spectrochim. Acta B 61, 1135–1140. https://doi.org/10.1016/j.sab.2006.07.005.

Ingram, B.L., 1970. Determination of fluoride in silicate rocks without separation of aluminium using a specific ion electrode. Anal. Chem. 42, 1825–1827. https://doi.org/10.1021/ac50160a067.

Jagner, D., Pavlova, V., 1972. A standard addition titration method for the determination of fluorine in silicate rocks. Anal. Chim. Acta 60, 153–158. https://doi.org/10.1016/S0003-2670(01)81894-8.

Klockenkämper, R., von Bohlen, A. (Eds.), 2015. Total-Reflection X-Ray Fluorescence Analysis and Related Methods. John Wiley & Sons Inc., Hoboken.

Krstajic, D., 2022. Application of Total Reflection X-Ray Fluorescence Analysis Down to Carbon. Diploma Thesis. Technische Universität Wien, Repositum. https://doi.org/10.34726/hss.2022.100800.

Kunther, W., Ferreiro, S., Skibsted, J., 2017. Influence of the ca/Si ratio on the compressive strength of cementitious calcium-silicate-hydrate binders. J. Mater. Chem. A 5, 17401. https://doi.org/10.1039/c7ta06104h.

Kuz'mina, T.G., Romashova, T.V., Troneva, M.A., Khokhlova, I.V., 2023. Experience of the determination of fluorine in rocks by X-ray fluorescence spectrometry. J. Anal. Chem. 78, 975–979. https://doi.org/10.1134/S1061934823080117.

Lin, M., Li, F., Li, X., Rong, X., Oh, K., 2023. Biochar-clay, biochar-microorganism and biochar-enzyme composites for environmental remediation: a review. Rev. Environ. Contam. Toxicol. 21, 1837–1862. https://doi.org/10.1007/s10311-023-01582-6.

Lopes, A.C., Martins, P., Lanceros-Mendez, S., 2014. Aluminosilicate and aluminosilicate based polymer composites: present status, applications and future trends. Prog. Surf. Sci. 89, 239–277. https://doi.org/10.1016/j.progsurf.2014.08.002.

Maltsev, A.S., Pashkova, G.V., Fernandez-Ruiz, R., Demonterova, E.I., Shuliumova, A.N., Umarova, N.N., Shergin, D.L., Mukhamedova, M.M., Chubarov, V.M., Mikheeva, E.A., 2021. Characterization of archaeological ceramics from eastern Siberia by total-reflection X-ray fluorescence spectrometry and principal component analysis. Spectrochim. Acta B 175, 106012. https://doi.org/10.1016/j.sab.2020.106012.

Maltsev, A.S., Umarova, N.N., Pashkova, G.V., Mukhamedova, M.M., Shergin, D.L., Panchuk, V.V., Kirsanow, D.O., Demonterova, E.I., 2023. Combination of total-reflection X-ray fluorescence method and chemometric techniques for provenance study of archaeological ceramics. Molecules 28, 1099. https://doi.org/10.3390/molecules28031099.

Martin, J.W., 2006. Glasses and ceramics. In: Martin, J.W. (Ed.), Materials for Engineering. Woodhead publishing limited, Cambridge, pp. 133–158. https://doi.org/10.1533/9781845691608.2.133.

Ndzana, G.M., Huang, Li, Wang, J.B., Zhang, Z.Y., 2018. Characteristics of clay minerals in soil particles from an argillic horizon of Alfisol in Central China. Appl. Clay Sci. 151, 148–156. https://doi.org/10.1016/j.clay.2017.10.014.

Okamoto, H., Sugiyama, Y., Nakano, H., 2011. Synthesis and modification of silicon nanosheets and other silicon nanomaterials. Chem-Eur. J. 17, 9864–9887. https://doi.org/10.1002/chem.201100641.

Prost, J., Wobrauschek, P., Streli, C., 2015. Comparison of different excitation modes for the analysis of light elements with a TXRF vacuum chamber. Powder Diffract. 30, 94–98. https://doi.org/10.1017/S088571561500024X.

Prost, J., Wobrauschek, P., Streli, C., 2018. Dual energy-band excitation from a low power Rh anode X-ray tube for the simultaneous determination of low Z and high Z elements (Na-U) using total-reflection X-ray fluorescence analysis (TXRF). Rev. Sci. Instrum. 89, 093108 https://doi.org/10.1063/1.5044527.

Sasamori, S., Meirer, F., Zöger, N., Streli, C., Kregsamer, P., Smolek, S., Mantler, C., Wobrauschek, P., 2009. Si wafer analysis of light elements by TXRF. ECS Trans. 25, 301–309. https://doi.org/10.1149/1.3204420.

Solé, V.A., Papillon, E., Cotte, M., Walter, P., Susini, J., 2007. A multiplatform code for the analysis of energy-dispersive X-ray fluorescence spectra. Spectrochim. Acta B 62, 63–68. https://doi.org/10.1016/j.sab.2006.12.002.

Streli, C., Aiginoer, H., Wobrauschek, P., 1989. Total reflection X-ray fluorescence analysis of low-Z elements. Spectrochim. Acta B 44. https://doi.org/10.1016/0584-8547(89)80055-2.

Streli, C., Aiginger, H., Wobrauschek, P., 1993. Light element analysis with a new spectrometer for total-reflection X-ray fluorescence. Spectrochim. Acta B 48. https://doi.org/10.1016/0584-8547(93)80020-U.

Streli, C., Wobrauschek, P., Ladisich, W., Rieder, R., Aiginger, H., 1995. Total reflection X-ray fluorescence analysis of light elements under various excitation conditions. X-Ray Spectrom. 24, 137–142. https://doi.org/10.1002/xrs.1300240310.

Streli, C., Wobrauschek, P., Bauer, V., Kregsamer, P., Görgl, R., Pianetta, P., Ryon, R., Pahlke, S., Fabry, L., 1997. Total reflection X-ray fluorescence analysis of light elements with synchrotron radiation and special X-ray tubes. Spectrochim. Acta B 52, 861–872. https://doi.org/10.1016/S0584-8547(96)01663-1.

Streli, C., Kregsamer, P., Wobrauschek, P., Gatterbauer, H., Pianetta, P., Pahlke, S., Fabry, L., Palmetshofer, L., Schmeling, M., 1999. Low Z total reflection X-ray fluorescence analysis – challenges and answers. Spectrochim. Acta B 54, 1433–1441. https://doi.org/10.1016/S0584-8547(99)00069-5.

Streli, C., Wobrauschek, P., Schraik, I., 2004. Comparison of SiLI detector and silicon drift detector for the determination of low Z elements in total reflection X-ray fluorescence. Spectrochim. Acta B 59, 1211–1213.

Wobrauscheck, P., Prost, J., Ingerle, D., Kregsamer, P., Misra, N.L., Streli, C., 2015. A novel vacuum spectrometer for total reflection X-ray fluorescence analysis with two exchangeable low power x-ray sources for the analysis of low, medium, and high Z elements in sequence. Rev. Sci. Instrum. 86, 083105 https://doi.org/10.1063/1.4928499.

Yahya, Z.N.M., Puspaseruni, N.P., Kurnia, R., Wahyuningrum, D., Mulyani, I., Wijanto, T., Kurihara, M., Waskito, S.S., Aslam, B.M., Marhaendrajana, T., 2022. The effect of aluminosilicate in the anionic-nonionic surfactant mixture on wetness and interfacial tension in its application for enhanced oil recovery. Energy Rep. 8, 1013–1025. https://doi.org/10.1016/j.egyr.2021.11.269.